Aus dem Zentrum für Augenheilkunde der Universität zu Köln
Klinik und Poliklinik für Allgemeine Augenheilkunde Direktor: Universitätsprofessor
Dr. med. C. Cursiefen

Quantifying Dermatochalasis Using 3-Dimensional Photogrammetry

Inaugural-Dissertation zur Erlangung der Doktorwürde
der Medizinischen Fakultät
der Universität zu Köln

vorgelegt von
Xueting Li
aus Jilin, China

promoviert am 10. Juni 2024

Gedruckt mit Genehmigung der Medizinischen Fakultät der Universität zu Köln

Druckjahr: 2024

Dekan: Universitätsprofessor Dr. med. G. R. Fink

1. Gutachter: Universitätsprofessor Dr. med. Dr. phil. L. Heindl

2. Gutachterin: Privatdozentin Dr. med. T. Schick

Erklärung

Ich erkläre hiermit, dass ich die vorliegende Dissertationsschrift ohne unzulässige Hilfe Dritter und ohne Benutzung anderer als der angegebenen Hilfsmittel angefertigt habe; die aus fremden Quellen direkt oder indirekt übernommenen Gedanken sind als solche kenntlich gemacht.

Bei der Auswahl und Auswertung des Materials sowie bei der Herstellung des Manuskriptes habe ich Unterstützungsleistungen von folgenden Personen erhalten:

Universitätsprofessor Dr. med. Ludwig M. Heindl, Dr. med. Alexander C. Rokohl, Dr. med. Yongwei Guo, Dr. med. Wanlin Fan.

Weitere Personen waren an der Erstellung der vorliegenden Arbeit nicht beteiligt. Insbesondere habe ich nicht die Hilfe einer Promotionsberaterin/eines Promotionsberaters in Anspruch genommen. Dritte haben von mir weder unmittelbar noch mittelbar geldwerte Leistungen für Arbeiten erhalten, die Zusammenhang mit dem Inhalt der vorgelegten Dissertationsschrift stehen.

Die Dissertationsschrift wurde von mir bisher weder im Inland noch im Ausland in gleicher oder ähnlicher Form einer anderen Prüfungsbehörde vorgelegt.

Die dieser Arbeit zugrunde liegenden Daten wurden durch meine Mitarbeit im Zentrum für Augenheilkundeder Universität zu Köln ermittelt.

Diese Daten wurden von Herrn Universitätsprofessor Dr. med. Ludwig M. Heindl, Herrn Dr. med. Alexander C. Rokohl, Herrn Dr. med. Yongwei Guo, Herrn Dr. med. Wanlin Fan und von mir zusammen ausgewertet.

Erklärung zur guten wissenschaftlichen Praxis:

Ich erkläre hiermit, dass ich die Ordnung zur Sicherung guter wissenschaftlicher Praxis und zum Umgang mit wissenschaftlichem Fehlverhalten (Amtliche Mitteilung der Universität zu Köln AM 132/2020) der Universität zu Köln gelesen habe und verpflichte mich hiermit, die dort genannten Vorgaben bei allen wissenschaftlichenTätigkeiten zu beachten und umzusetzen.

Köln, den 15.07.2024

Unterschrift: Xueting Li

ACKNOWLEDGEMENTS

I would like to express my heartfelt gratitude and appreciation to my supervisor Univ. - Prof. Dr. Dr. Ludwig M. Heindl, whose guidance, expertise, and unwavering support have been instrumental in shaping this thesis. His commitment to academic excellence, patience, and insightful feedback have challenged me to delve deeper into my research and have greatly enhanced the quality of this work. I am truly grateful for his mentorship and the invaluable lessons I have learned under his guidance.

I am also grateful to Dr. med. Alexander C. Rokohl, for his valuable insights, critical evaluation, and constructive suggestions throughout my doctoral study. His instructions and encouragement have been essential in keeping me motivated and inspired.

My sincere gratitude goes to my colleagues Yongwei Guo, Wanlin Fan, Sitong Ju, Xiaojun Ju, and Xincen Hou and fellow researchers who have supported me during this journey. Their stimulating discussions, collaboration, and exchange of ideas have broadened my perspectives and inspired me to push the boundaries of knowledge.

I would like to acknowledge the financial support provided by Chinese Scholarship Council. Their investment in my research has not only facilitated the completion of this thesis but has also enabled me to attend conferences, present my work, and engage with experts in my field.

Lastly, I would like to express my gratitude to my parents and my husband Dr. Chen Song for their unwavering support, encouragement, and understanding throughout this challenging and rewarding journey. Their love, patience, and belief in me have been a constant source of strength and motivation.

Although it is impossible to name everyone who has contributed to my doctoral thesis, I extend my sincere appreciation to all those whose influence and support have shaped my academic and

personal growth. Their support has made this accomplishment possible, and for that, I am truly grateful.

Dedication

To my family and friends

Contents

Abbreviations

Abbreviation	Full Form
MRD	marginal reflex distance
Three-dimensional	3D
UPML	upper palpebral margin length
LPML	lower palpebral margin length
CT	canthal tilt
PFH	palpebral fissure height
PFW	palpebral fissure width
FPD	fold-palpebral margin distance
PFI	palpebral fissure index
CPBH	central-brow pupil height
MPBH	medial palpebral fissure to brow height
LPBH	lateral palpebral fissure to brow height
AI	artificial intelligence

1. Summary

The main objectives of this study, titled "Quantifying Dermatochalasis Using 3-Dimensional Photogrammetry" [1], are to characterize patients with dermatochalasis. The results were obtained by analyzing periocular features in 145 dermatochalasis patients using standardized 3D imaging provided by the VECTRA M3 3D imaging system. Dermatochalasis typically affects both eyes simultaneously, and the relationships between PFW, LPML, and age were discovered.

We conducted an analysis involving various clinical measurements, including palpebral fissure height (PFH), palpebral fissure width (PFW), upper lid fold-palpebral margin distance (FPD), upper palpebral margin length (UPML), lower palpebral margin length (LPML), canthal tilt (CT), palpebral fissure index (PFI), upper eyelid area, and ocular surface area. The 145 participants were all Caucasian, comprising 48 males and 97 females, aged between 35 and 91 years. The analysis revealed that among males, there were no significant differences in parameters. In the female group, the left-side PFH was slightly larger than the right-side PFH ($P = 0.023$), but the difference was less than 1 mm. The corresponding PFI also exhibited a difference in the female group ($P = 0.009$). Gender differences analysis indicated that PFH and PFW measurements were significantly greater in males (9.680 ± 1.542 mm, 27.146 ± 2.689 mm, respectively) than in females (8.995 ± 1.494 mm, 25.884 ± 2.913 mm, respectively) (both $P < 0.001$). However, males had a shorter FPD (2.470 mm [3.658]) than females (3.051 mm [3.922]). Additionally, the male group had longer eyelids (UPML 35.830 ± 4.342 mm; LPML 29.762 ± 3.277 mm) than females (UPML 33.622 ± 4.417 mm; LPML 28.474 ± 3.246 mm). Furthermore, the exposed ocular surface area in males was greater than in females (2.069 ± 0.515 mm² and 1.895 ± 0.483 mm², respectively), and the male upper eyelid area (5.236 ± 1.179 mm²) was smaller than that of females (6.153 ± 1.382 mm²). Additionally, PFW ($R = -0.523$, $p < 0.001$) decreased moderately with age among males. The correlation between UPML and age was weak ($R = -0.367$, $P = 0.010$). Among females, moderate correlations were found between age and PFW ($R = -0.566$, $P <$

0.001) and LPML (R = -0.537, P < 0.001). PFH (R = -0.315, P = 0.002), UPML (R = -0.381, P < 0.001), and ocular surface area (R = -0.457, P < 0.001) showed weak correlations with age.

Understanding age-related changes in the periocular region is crucial for planning surgical procedures. It highlights the need to consider both age and sex-related factors when formulating treatment plans for dermatochalasis patients in the future. When assessing patients with eyelid skin laxity, it's essential to evaluate the condition of their inner and outer canthal ligaments. During blepharoplasty, special attention should be paid to the skin near the lateral canthus, and the amount of resection may need adjustment. Furthermore, as patients age, it becomes increasingly important to focus on postoperative complications, particularly lower eyelid malposition.

This study demonstrates age-related alterations in Caucasians, with significant variations across ages and sexes in periocular characteristics. Undoubtedly, similar discrepancies exist in other races. Further investigation and clinical data collection will be necessary for enhanced surgical planning.

2. Zusammenfassung

Das Hauptziel dieser Studie mit dem Titel „Quantifying Dermatochalasis Using 3-Dimensional Photogrammetry“ [1] besteht darin, Patienten mit Dermatochalasis zu charakterisieren. Die Ergebnisse wurden durch die Analyse periokularer Merkmale bei 145 Dermatochalasis-Patienten mithilfe einer standardisierten 3D-Bildgebung des VECTRA M3 3D-Bildgebungssystems erzielt. Dermatochalasis betrifft typischerweise beide Augen gleichzeitig, und es wurden Zusammenhänge zwischen PFW, LPML und dem Alter entdeckt.

Wir führten eine Analyse mit verschiedenen klinischen Messungen durch, darunter Lidspaltenhöhe (PFH), Lidspaltenbreite (PFW), Abstand zwischen Oberlidfalte und Lidrand (FPD), Länge des oberen Lidrands (UPML) und Länge des unteren Lidrands (LPML), Lidneigung (CT), Lidspaltenindex (PFI), Oberlidbereich und Augenoberfläche. Die 145 Teilnehmer waren alle Kaukasier, darunter 48 Männer und 97 Frauen im Alter zwischen 35 und 91 Jahren.

Die Analyse ergab, dass es bei Männern keine signifikanten Unterschiede in den Parametern gab. In der weiblichen Gruppe war der PFH auf der linken Seite etwas größer als der PFH auf der rechten Seite ($P = 0,023$), aber der Unterschied betrug weniger als 1 mm. Auch der entsprechende PFI zeigte einen Unterschied in der weiblichen Gruppe ($P = 0,009$). Die Analyse der Geschlechtsunterschiede ergab, dass die PFH- und PFW-Messungen bei Männern signifikant größer waren (9,680 ± 1,542 mm bzw. 27,146 ± 2,689 mm) als bei Frauen (8,995 ± 1,494 mm bzw. 25,884 ± 2,913 mm) (beide $P < 0,001$). Allerdings hatten Männer einen kürzeren FPD (2,470 mm [3,658]) als Frauen (3,051 mm [3,922]). Außerdem hatte die männliche Gruppe längere Augenlider (UPML 35,830 ± 4,342 mm; LPML 29,762 ± 3,277 mm) als die weiblichen (UPML 33,622 ± 4,417 mm; LPML 28,474 ± 3,246 mm). Die freiliegende Augenoberfläche war bei Männern größer als bei Frauen (2,069 ± 0,515 mm^2 bzw. 1,895 ± 0,483 mm^2), und die männliche Oberlidfläche (5,236 ± 1,179 mm^2) war kleiner als die bei Frauen (6,153 ± 1,382 mm^2).

Darüber hinaus nahm das PFW ($R = -0,523$, $p < 0,001$) bei Männern mit dem Alter moderat ab. Die Korrelation zwischen UPML und Alter war schwach ($R = -0,367$, $P = 0,010$). Bei den Frauen wurden moderate Korrelationen zwischen Alter und PFW ($R = -0,566$, $P < 0,001$) und LPML ($R = -0,537$, $P < 0,001$) gefunden. PFH ($R = -0,315$, $P = 0,002$), UPML ($R = -0,381$, $P < 0,001$) und Augenoberfläche ($R = -0,457$, $P < 0,001$) zeigten schwache Korrelationen mit dem Alter.

Das Verständnis altersbedingter Veränderungen im Periokularbereich ist für die Planung chirurgischer Eingriffe von entscheidender Bedeutung. Es unterstreicht die Notwendigkeit, bei der künftigen Formulierung von Behandlungsplänen für Dermatochalasis-Patienten sowohl alters- als auch geschlechtsbezogene Faktoren zu berücksichtigen. Bei der Beurteilung von Patienten mit schlaffer Augenlidhaut ist es wichtig, den Zustand ihrer inneren und äußeren Lidbänder zu beurteilen. Bei der Blepharoplastik sollte besonderes Augenmerk auf die Haut in der Nähe des seitlichen Augenwinkels gelegt werden, und das Ausmaß der Resektion muss möglicherweise angepasst werden. Außerdem wird es mit zunehmendem Alter der Patienten immer wichtiger, sich auf postoperative Komplikationen zu konzentrieren, insbesondere auf die Fehlstellung des unteren Augenlids.

Diese Studie zeigt altersbedingte Veränderungen bei Kaukasiern mit erheblichen Unterschieden zwischen Alter und Geschlecht in den periokularen Merkmalen. Zweifellos gibt es ähnliche Unterschiede auch bei anderen Rassen. Für eine verbesserte chirurgische Planung sind weitere Untersuchungen und die Erfassung klinischer Daten erforderlich.

3. Introduction

3.1 Dermatochalasis

Aging is a complex process that impacts various aspects of the body, including the bony skeleton, muscles, fat, and the skin surrounding the orbit and its structures. The facial skeleton undergoes resorption, leading to the retrusion of the periosteum. Consequently, the positions of facial ligaments and muscles shift due to the movement of the periosteum. The aging process in the orbit results in hollowing, folds becoming more prominent, protrusion of fat pads, and deterioration of skin texture. Orbital rim resorption is uneven; specifically, the inferolateral and superomedial quadrants of the orbit recede with age, while the central parts of the superior and inferior orbital rims remain relatively stable [2].

The upper eyelid and lower eyelid consist of anterior, middle, and posterior layers. The anterior layer is composed of the skin of the eyelid and the orbicularis oculi muscle, while the posterior layer refers to the levator palpebrae superioris, superior or inferior tarsal muscle, tarsal plate, and conjunctiva. Dermatochalasis, or sagging eyelids, is a common condition characterized by the excess skin and muscle laxity of the eyelids (Figure 1). The overall prevalence of dermatochalasis (moderate and severe sagging eyelids) in individuals over 45 years old is reported to be 17.8%. Age, male gender, lighter skin tone, and higher body mass index are considered significant and independent risk factors [3]. Apart from causing concerns about one's appearance, dermatochalasis can lead to functional issues. Some patients with dermatochalasis experience limited vision, visual fatigue, or even eyelid problems such as entropion, trichiasis, and ectropion [4].

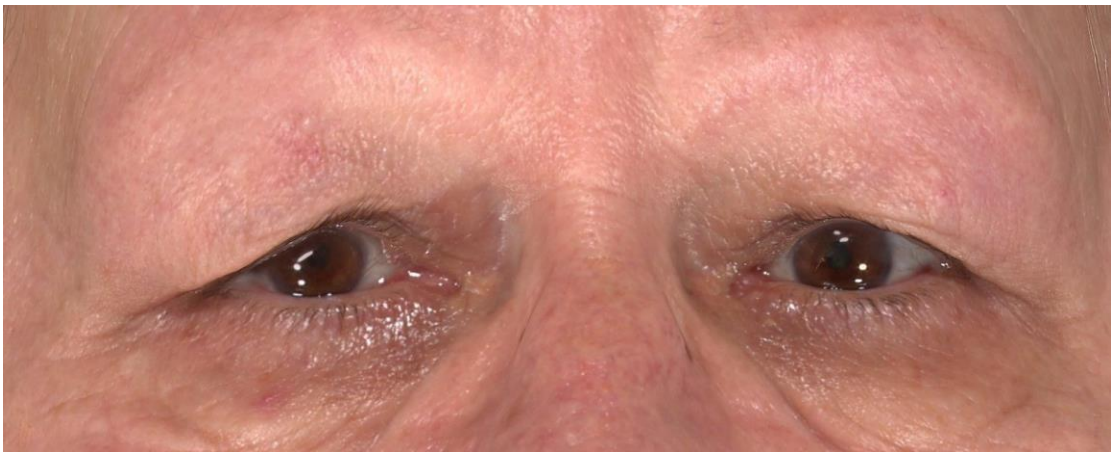

Figure 1. Dermatochalasis Patients Captured Using the VECTRA M3 Imaging System

3.2 Facial anthropometry

Before the blepharoplasty, the surgeon obtains the detailed clinical history of the patient, clinical evaluation, and the aesthetic evaluation is also essential for all patients, involving considerations such as brow asymmetry, upper eyelid measurements, and the amount and location of excess orbital fat. Precise measurements of the eyelids and their surrounding structures are paramount. These measurements, which include parameters like marginal reflex distance 1 (MRD-1), MRD-2, FPD, PFH, PFW and brow line height, are vital. They not only help characterize eyelid and ocular surface features but also play a significant role in evaluating facial appearance. These measurements offer valuable quantitative data for both preoperative and postoperative assessments.

Since as early as 1921, facial measurements have been taken using manual anthropometry techniques involving calipers, cephalometric rulers, and other ancient analog devices [5]. Manual anthropometry was once considered the gold standard for facial measurements due to its non-invasive nature and low cost. However, this method is time-consuming and exhibits poor intra-rater reliability [6]. In recent times, manual anthropometry is being rapidly replaced by advanced digital technology devices.

Currently, two-dimensional (2D) photos are widely employed to calculate distances,

angles, and even areas based on pre-placed marks. Some studies have shown that 2D photogrammetry is comparable to direct measurement and may serve as a viable alternative [7]. However, research by Lim et al. [8] revealed that certain measurements, such as bigonial breadth, bizygomatic breadth, and head breadth, cannot be reliably and accurately measured using 2D photogrammetry. Another study by Ayaz et al. [9]. demonstrated that 2D photogrammetry exhibited the highest overall combined error for linear measurements compared to traditional anthropometry methods. This inaccuracy can be attributed to subjective analysis, magnification errors, parallax, variations in lighting, and differences in head orientation.

Considering these challenges, 2D photogrammetry may serve as a supplement to direct manual anthropometry rather than a complete replacement. While it offers significant advantages, it is essential to acknowledge its limitations and potential errors in certain measurements.

3.3 Stereophotogrammetry

In 1987, the Loughborough Anthropometric Shade Scanner (LASS) was designed and developed to automate anthropometry [10]. In the subsequent decades, advancements in stereophotogrammetry have enabled the clinical implementation of three-dimensional (3D) imaging. Stereophotogrammetry exists in various forms, and several studies have assessed the clinical use of 3D stereophotogrammetric imaging systems, including the Vectra H1-270 camera (Canfield Imaging Systems, Fairfield, NJ, USA) [11], 3D Vectra® H1 (Canfield Scientific Inc., Parsippany, NJ, USA) [9], Vectra H2 (Canfield Imaging, Parsippany, NJ, USA) [12, 13], and the 3dMD head system (3dMD LLC, Atlanta, GA, USA) [14]. Some studies have also demonstrated that facial scanning can be achieved using smartphone applications [15, 16].

The VECTRA M3 3D imaging system (Canfield Scientific, Inc., Parsippany, NJ, USA) (Figure 2) features a 1.2mm geometry resolution (triangle edge length) capture system, ensuring photorealistic rendering of the finest details. Additionally, the capture time is

only 3.5 milliseconds, requiring minimal patient cooperation. In our group's previous studies, we validated the high reliability of the VECTRA M3 3D imaging system in the periocular region. This was achieved by identifying 52 periocular landmarks on fifty-one 3D images of Caucasian individuals. We further evaluated 49 corresponding linear, curvilinear, and angular measurements, and the results demonstrated excellent intra-rater and inter-rater reliability [17]. Additionally, we placed five commonly used statistical indicators at seven periocular positions, including the endocanthion and the upper medial, upper middle, upper lateral, lower medial, lower middle, and lower lateral eyelids, to confirm the reliability of area measurements in the periocular region using the VECTRA M3 3D imaging system [18]. In our recently published studies, we also highlighted the limitations of volumetric measurements based on a single image [19, 20].

Figure 2. VECTRA M3 dimensions [53]

3.4 Blepharoplasty

Blepharoplasty stands out as one of the most frequently performed surgeries for upper

eyelid rejuvenation. The term itself is derived from the Greek words "blepharo," meaning eyelid, and "plasso," meaning to shape or form. Classic indications for blepharoplasty surgery include upper eyelid skin redundancy, the absence of an upper eyelid fold, and senile or subclinical ptosis. In traditional blepharoplasty, fundamental surgical procedures involve removing excess skin, excising surplus orbicularis oculi muscle, eliminating retroseptal fat, and employing various canthopexy and canthoplasty techniques as needed. Modern blepharoplasty techniques not only focus on reduction but also encompass the restoration of deflated tissues, atrophied fat, and muscle laxity through various methods. There has been widespread acceptance of the conservative excision of eyelid structures [21]. But the limit between over-resection and under-resection is difficult to be determined. The undersection can result in residual eyelid fat or skin postoperatively.

3.4.1 Preoperative evaluation

Before surgery, engaging in detailed discussions with patients to fully understand their expectations is crucial. Patients must be informed about potential complications that may arise. Surgeons should work to dispel any unrealistic expectations and ensure that patients make well-informed decisions. Following this, a comprehensive examination of ocular and systemic conditions is conducted, including assessments of visual acuity, the bell phenomenon test, lacrimal function (such as the Schirmer test, tear film breakup, rose bengal staining, and tear lysozyme). The surgeon also reviews patients' anticoagulant/antiplatelet therapy or medication history. In addition to obtaining detailed clinical history, clinical evaluation, and preoperative photography, the surgeon assesses patients' brow asymmetry and determines if they have compensated brow ptosis for aesthetic evaluation. Any redundant skin of the upper eyelid is pointed out to patients and documented, including any asymmetries.

3.4.2 Operative treatment

Patients were instructed to prepare thoroughly, including the removal of all makeup.

The surgeon marked the incision lines with the patient in an upright position, providing a guideline for the subsequent incision. The key steps were as follows: (1) Anesthesia: Patients received either local anesthesia, local anesthesia with conscious sedation, or general anesthesia based on their condition and the surgeon's preference. (2) Excision and Dissection: The surgeon made incisions following the reference of the markings, excising skin and, if necessary, the orbicularis oculi strip. (3) Fat Resection: Conservative fat excision was performed to achieve a natural fullness without heaviness of the eyelid. (4) Suturing: The lacrimal gland was assessed, and then the skin was closed.

3.4.3 Postoperative management

After the operation, the patient's operative eye was ice-packed, and prophylactic antibacterial eye drops were administered. Sutures were removed during the first week after the surgery. Patients returned for follow-up appointments at one week, 1 month, and 3 months after the surgery. During these appointments, various examinations, including visual acuity, pupil examination, intraocular pressure measurement, and follow-up 3D photos, were conducted. The pre-intra-post-operative clinical pathway is shown as Figure 3.

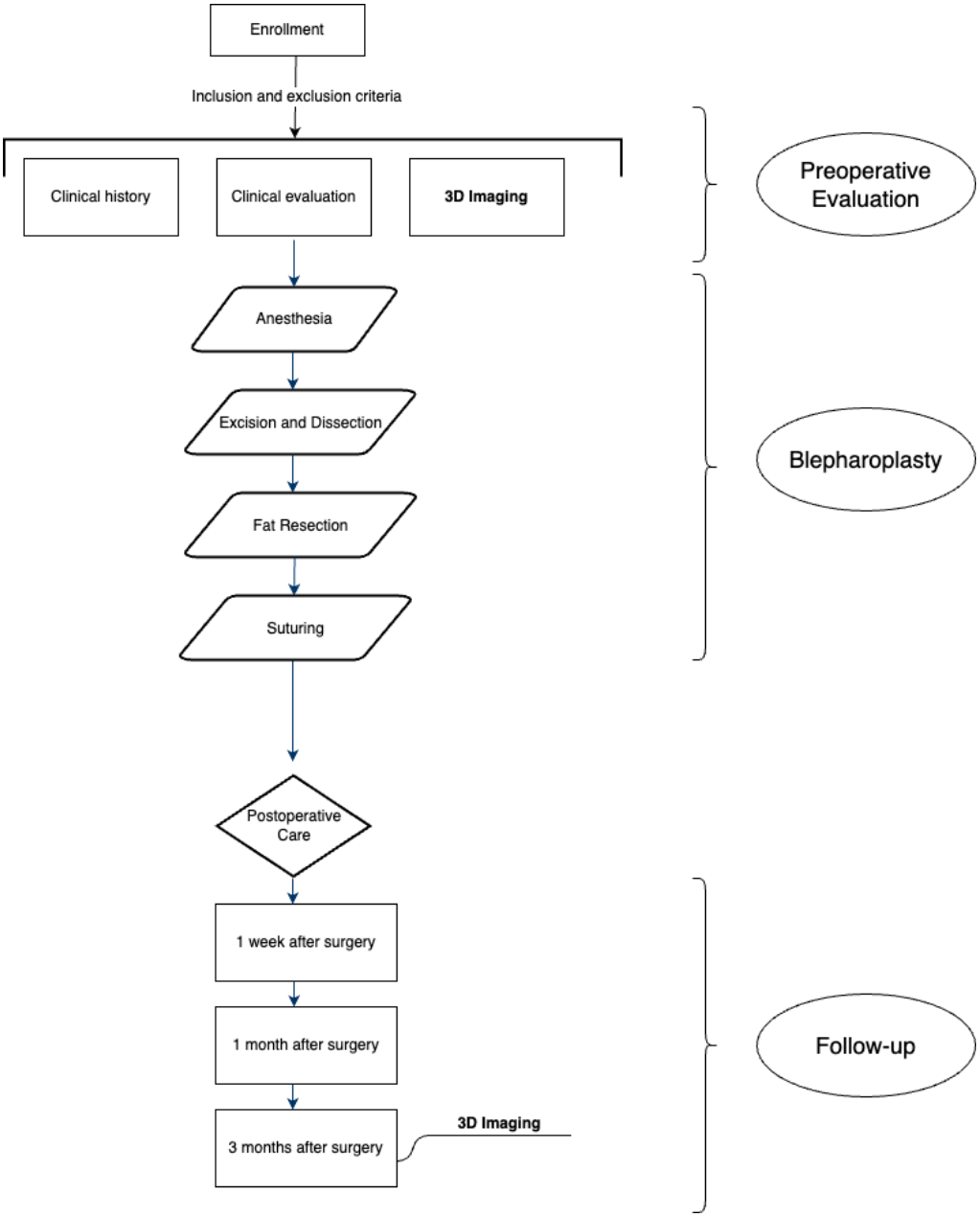

Figure 3. Pre-intra-post-operative clinical pathway.

Prior to surgery, patients underwent detailed consultations for clinical history, clinical evaluation, and 3D imaging. The blepharoplasty procedure involved anesthesia, excision and dissection, fat resection, and suturing. After surgery, patients received careful postoperative care and were scheduled for follow-up appointments at 1 week, 1 month, and 3 months post-surgery. Additionally, 3D photos were taken during the 3-month period after the surgery.

3.5 Non-surgical Approach

Blepharoplasty is often the first choice to provide radical and long-term results, especially in severe cases. At the same time, numerous non-surgical methods are becoming an increasingly interesting alternative for the treatment of dermatochalasis, e.g., lasers, hyaluronic acid (HA) fillers, and plasma exeresis. These advancements are providing viable options for cosmetic eyelid treatments.

The CO_2 laser, frequently utilized in blepharoplasty, offers bloodless incisions, and boasts rapid and precise properties. Laser-assisted blepharoplasty has significantly improved the treatment of patients with varying degrees of eyelid and periocular aging, minimizing downtime [22]. While the laser-assisted technique offers numerous advantages, it's important to note that the heat conduction induced by the laser cannot be completely avoided, potentially contributing to scarring [23]. In the early postoperative period, some patients can also experience erythema, edema, and hyperpigmentation especially when undergoing laser skin resurfacing. These viewpoints stem from the experiences and personal observations of surgeons who have practiced both techniques. A unanimous consensus has not yet been reached. Nevertheless, laser-assisted surgery could be a safe and effective option, especially when the surgeon is experienced, knowledgeable about laser tissue interactions, and in cases where transconjunctival blepharoplasty is more suitable [24].

In addition, Romeo et al. [25, 26] compared HA filling with blepharoplasty surgery in 500 patients (including 382 patients were treated with HA injections, 45 patients both with blepharoplasty surgery and HA filling, whereas only 73 patients underwent surgery), and draw the conclusion that HA fillers can be used alone or in conjunction with blepharoplasty to restore upper eyelid volume loss. For the plasma exeresis, Verner et al. [27] reported that it was an effective and safety method in dermatochalasis treatment. Rossi et al. [28] suggested that plasma exeresis could be a valid solution for eyelid dermatochalasis; however, further studies are required.

3.6 Aims

This study aimed to quantify the periocular characteristics of dermatochalasis patients using standardized 3D imaging and to compare age and sex-related changes in periocular features.

Aesth Plast Surg
https://doi.org/10.1007/s00266-023-03738-9

Quantifying Dermatochalasis Using 3-Dimensional Photogrammetry

Xueting Li[1] · Alexander C. Rokohl[1,2] · Wanlin Fan[1] · Michael Simon[1,2] · Xiaojun Ju[1] · Till Rosenkranz[1] · Philomena A. Wawer Matos[1,2] · Yongwei Guo[3] · Ludwig M. Heindl[1,2]

Received: 2 July 2023 / Accepted: 20 October 2023

Abstract

Background Creating an appropriate treatment plan for patients with dermatochalasis requires careful investigation of the periocular region. Utilizing photographic documentation can assist physicians in conducting preoperative analysis and managing expectations regarding surgical outcomes.

Objectives This study aimed to quantify the periocular characteristics of dermatochalasis patients using standardized 3D imaging and to compare age and sex-related changes in periocular features.

Methods In this cross-sectional study, we recruited 145 Caucasian patients with periocular dermatochalasis, comprising 48 men and 97 women, aged between 35 and 91 years. Standardized three-dimensional facial photographs were taken using the 3D Imaging system VECTRA M3. Linear dimensions, curve length, angle, indices, and sizes were measured and analyzed, including palpebral fissure height (PFH), palpebral fissure width (PFW), upper lid fold-palpebral margin distance (FPD), upper palpebral margin length (UPML), lower palpebral margin length (LPML), canthal tilt (CT), palpebral fissure index (PFI), upper eyelid area, and ocular surface area.

Results In the female group, the left-side PFH was slightly larger than the right-side PFH ($P = 0.023$), but the difference was less than 1mm. The corresponding PFI also showed a difference in the female group ($P = 0.009$). Statistically significant differences were shown in genders for specific parameters, except PFI ($P = 0.251$) and CT ($P = 0.098$). Among males, PFW ($R = -0.523$, $p < 0.001$) and LPML ($R = -0.514$, $P = 0.264$) decreased moderately with age. The correlation between UPML and age was weak ($R = -0.367$, $P = 0.010$). Similarly, among females, moderate correlations were found between age and PFW ($R = -0.566$, $P < 0.001$) and LPML ($R = -0.537$, $P < 0.001$). Additionally, PFH ($R = -0.315$, $P = 0.002$), UPML ($R = -0.381$, $P < 0.001$), and ocular surface area ($R = -0.457$, $P < 0.001$) showed weak correlations with age.

Conclusions The study found that dermatochalasis usually affects both eyes simultaneously, and age is a significant factor in the morphological changes of certain periocular features regardless of sex. The PFI is not influenced by age or sex. These findings may provide useful information for surgical planning and understanding age-related changes in the periocular area.

Level of Evidence V This journal requires that authors assign a level of evidence to each article. For a full description of these Evidence-Based Medicine ratings, please refer to the Table of Contents or the online Instructions to Authors www.springer.com/00266.

Keywords Dermatochalasis · Periocular morphology · Age · Anthropometry · Three-dimensional imaging

✉ Yongwei Guo
yongwei-guo@zju.edu.cn

✉ Ludwig M. Heindl
ludwig.heindl@uk-koeln.de

[1] Department of Ophthalmology, University of Cologne, Faculty of Medicine and University Hospital Cologne, Kerpener Straße 62, 50937 Cologne, Germany

[2] Center for Integrated Oncology (CIO), Aachen-Bonn-Cologne-Duesseldorf, Cologne, Germany

[3] Eye Center, The Second Affiliated Hospital, School of Medicine, Zhejiang University, Zhejiang Provincial Key Laboratory of Ophthalmology, Zhejiang Provincial Clinical Research Center for Eye Diseases, Zhejiang Provincial Engineering Institute on Eye Diseases, Hangzhou, Zhejiang, China

Published online: 09 November 2023

Introduction

A person's appearance and how they are perceived affect social interactions. The periocular region, which is strongly associated with facial attractiveness, is particularly susceptible to showing signs of aging that are often considered less attractive. Dermatochalasis is an advanced form of skin aging that affects the periocular region, manifesting as laxity and thinning of the skin as well as atrophy of the periocular soft tissue that may result in anatomical misalignment and formation of rhytides. Colloquially referred to as "baggy eyes," dermatochalasis is often considered a cosmetic problem that affects middle-aged and older individuals.

Blepharoplasty was developed to enhance the attractiveness of the periocular region and to achieve periocular rejuvenation [1]. Prior to performing surgery on patients with dermatochalasis, photographic documentation and careful, detailed evaluation of the patient's facial features are essential to create an appropriate treatment plan; any potential asymmetry should be identified and discussed with the patient. However, accurate evaluation of facial features can be challenging due to differences in photograph sizes, head movements, and facial expressions.

To overcome these challenges, noninvasive 3D imaging technology that detects facial landmarks and measures a series of variables is used to record and analyze variations in the periocular region [2–6]. In previous studies, we found that the intrarater measurements exhibited the highest reliability, followed by the interrater and intramethod measurements [7]. These findings validated the method's reliability for 3D linear and areal measurements in the periocular region and identified the limitations in the reliability of volumetric measurements derived from direct measurements using a single image [4, 8]. Additionally, the pupil has been verified as the most stable landmark for establishing reference planes to describe periocular changes [9]. However, no 3D imaging technology-based studies have been conducted on patients with dermatochalasis. Therefore, our study aimed to analyze the periocular characteristics of patients with dermatochalasis before surgery and evaluate the impact of age and sex furtherly.

Methods

Participants and Recruitment

We recruited patients diagnosed with dermatochalasis between January 2022 and April 2023 at REDACTED. Each participant was of Caucasian ethnicity, aged over 18 years, and had no history of eyelid disease, trauma, or surgery that could have impacted their facial morphology. Individuals with cognitive deficits or those who were unwilling or unable to cooperate were excluded. The study was conducted in accordance with the Declaration of Helsinki (as revised in 2013). The study was approved by the Ethics Committee of REDACTED (approval number: 17–199) and informed consent was taken from all individual participants.

Acquisition of Three-dimensional Facial Images

Stereophotography was performed using the VECTRA M3 3D Imaging System (Canfield Scientific, Inc., Parsippany, NJ, USA). The 3D camera was calibrated daily, and a trained operator (X.L.) captured all images following the manufacturer's guidelines. All images were captured in the same clinical photography room under standard ambient lighting without natural light sources. Patients were instructed to remove glasses, masks, and any other facial coverings, including facial makeup. Six cameras were located at a fixed distance and angle relative to the patient. Patients were seated in a fixed position and instructed to maintain neutral expression while looking directly into a mirror located in the upper middle region of the machine, keeping their eyes between the vertical and horizontal reference lines on the screen. Standard patient images were obtained, and all measurements and analyses were performed by the same operator (X. L.). Finally, proprietary image processing software Vectra® M3 (3D Imaging System; Canfield Scientific, Parsippany, NJ, USA) was used to measure and analyze the 3D facial models. A series of standardized landmarks in the periocular region was selected based on previously published studies [3, 4]. These landmarks are shown in frontal (Fig. 1A) and lateral (Fig. 1B) views, with their respective abbreviations defined in Table 1.

Additionally, we measured and calculated the palpebral fissure height (PFH), palpebral fissure width (PFW), upper lid fold-palpebral margin distance (FPD), curve length of the upper palpebral margin length (UPML), curve length of the lower palpebral margin length (LPML), angle of canthal tilt (CT), palpebral fissure index (PFI), upper eyelid surface area, and ocular surface area by clicking to connect the corresponding landmarks (Table 2).

Statistical Analysis

The Kolmogorov–Smirnov test for normality was used to evaluate the distribution of the data. Demographic and clinical characteristics are presented as mean ± standard

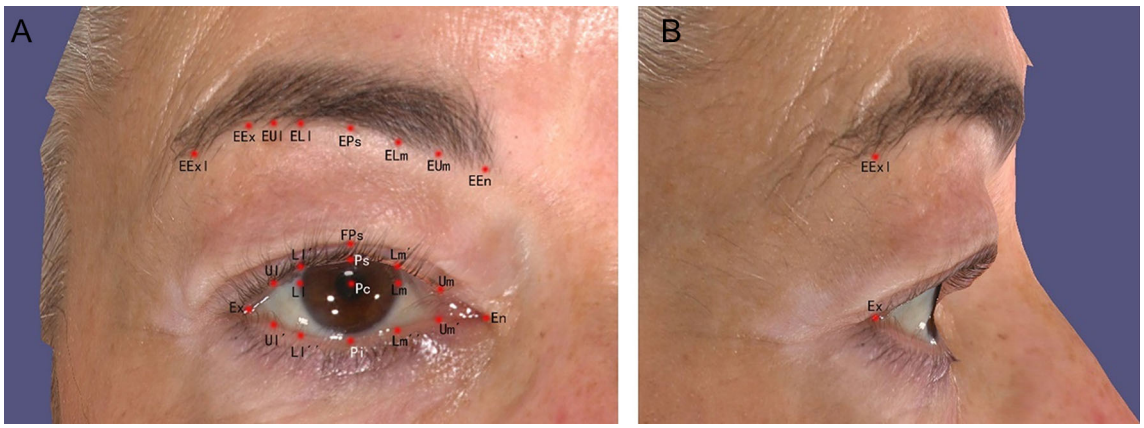

Fig. 1 The standardized landmarks of three-dimensional evaluation. **A** The frontal view of the periocular region; **B** The lateral view of the periocular region. Pc is the pupillary center. Lm and Ll are corneoscleral limbus point horizontal to Pc. Vertical to Pc are correspondent points, i.e., Eps, FPs, Ps, and Pi. Similarly, Elm, Lm', Lm'' are vertical to Lm, and ELl, Ll'', as well as Ll' are vertical to Ll. Um is the middle point between Endocanthion (En) and Lm', and Ul is the middle point between Exocanthion (Ex) and Ll' at the upper palpebral margin on the lash roots. Likewise, Ul' and Um' are marked at the lower palpebral margin on the lash roots. Furthermore, EUm is vertical to Um, EEx is vertical to Ul, EEn is vertical to En, and EEx is also vertical to Ex at the inferior margin of eyebrows. EExl is vertical to Ex at the inferior margin of the eyebrow in the lateral review.

Table 1 Definition of abbreviations of periocular landmarks

Abbreviation of landmarks	Definition
En	Endocanthion, inner commissure of the palpebral fissure
Ex	Exocanthion, outer commissure of the lower and upper eyelash roots of the palpebral fissure
Pc	pupillary center
Ps	Palpebrae superioris, Point vertical to Pc at the upper palpebral margin on the lash roots
Pi	Palpebrae inferioris, Point vertical to Pc at the lower palpebral margin on the lash roots
FPs	Point vertical to Pc at the lid fold superioris
EPs	Point vertical to Pc at the inferior margin of eyebrows
Lm	Medial corneoscleral limbus point horizontal to pupillary center
Lm'	Point vertical to Lm at the upper palpebral margin on the lash roots
Lm''	Point vertical to Lm at the lower palpebral margin on the lash roots
Um	Middle point between En and Lm´ at the upper palpebral margin on the lash roots
Um'	Middle point between En and Lm´´ at the lower palpebral margin on the lash roots
Ll	Lateral corneoscleral limbus point horizontal to pupillary center
Ll'	Point vertical to Ll at the upper palpebral margin on the lash roots
Ll''	Point vertical to Ll at the lower palpebral margin on the lash roots
Ul	The middle between Ex and Ll´ at the upper palpebral margin on the lash roots
Ul'	The middle between Ex and Ll´´ at the lower palpebral margin on the lash roots
EEn	Point vertical to En at the inferior margin of eyebrows
EEx	Point vertical to Ex at the inferior margin of eyebrows
EExL	Point vertical to Ex at the inferior margin of eyebrow in the lateral review
EUm	Point vertical to Um at the inferior margin of eyebrows
ELm	Point vertical to Lm at the inferior margin of eyebrows
ELl	Point vertical to Ll at the inferior margin of eyebrows
EUl	Point vertical to Ul at the inferior margin of eyebrows

Adapted by permission from Springer Nature from Guo Y et al. Reliability of periocular anthropometry using three-dimensional digital stereophotogrammetry. Graefes Arch Clin Exp Ophthalmol 2019; 257:2517–31

Table 2 Definition of linear distance, curve, and size measurement variables for the periocular region

Abbreviation	Landmarks
Linear dimensions	
Palpebral fissure height, PFH	Ps-Pi
Palpebral fissure width, PFW	En-Ex
Upper lid fold-palpebral margin distance, FPD	Ps-FPs
Curve length	
Upper palpebral margin length, UPML	En-Um-Lm'-Ps-Ll'-Ul-Ex
Lower palpebral margin length, LPML	En-Um'-Lm''-Pi-Ll''-Ul'-Ex
Angle	
Canthal tilt, CT	Ex(l)-En(l)-En(r), or Ex(r)-En(r)-En(l)
Indices	
Palpebral fissure index, PFI	PFH/PFW
Sizes	
Upper eyelid area	EEn-EUm-ELm-EPs-ELl-EUl-EEx-EExl-Ex-Ul-Ll'-Ps-Lm'-Um-En-EEn
Ocular surface area	En-Um-Lm'-Ps-Ll'-Ul-Ex-Ul'-Ll''-Pi-Lm''-Um'-En

Adapted by permission from Springer Nature from Guo Y et al. Reliability of periocular anthropometry using three-dimensional digital stereophotogrammetry. Graefes Arch ClinExp Ophthalmol 2019; 257:2517–31

deviation (or median and interquartile intervals). Paired sample *t*-tests were conducted to compare bilateral eyes, and independent samples *t*-tests were performed for normally distributed data to compare different sexes. Wilcoxon signed-rank tests and Mann–Whitney U tests were employed for data that were not normally distributed. Pearson correlation coefficient was used for correlation analysis. The statistical analyses were conducted using SPSS software version 22 (IBM Corporation, Armonk, NY, USA). Figures were generated using GraphPad Prism 8.0.1 (GraphPad Software, San Diego, CA, USA). *P* values ≤ 0.05 were considered statistically significant.

Results

A total of 145 participants with dermatochalasis were enrolled in our study, ranging from 35 to 91 years of age (mean age of 59.120 ± 9.282 years). There were 290 eyes in 48 men (33.103%) and 97 women (66.897%).

Differences in Bilateral Periocular Area

Patients' right eyes were compared with their corresponding left eyes (Table 3). The PFH of the left eye was found to be greater than that of the right eye both in the total group and in the female group. Correspondingly, the PFI also differed significantly between the two sides, with the left eye showing higher values than the right eye in women. However, the remaining parameters, including PFW, FPD as well as the curve length of UPML and LPML, CT angles, upper eyelid area, and ocular surface area did not show any difference between the two sides.

Differences Between Male and Female Patients

We also examined discrepancies between male (mean age of 61.420 ± 8.865 years) and female (mean age of 58.680 ± 9.362 years) patients (Table 4). There was no significant difference in patients' age according to sex; however, several characteristics differed significantly between the male group and the female group. Specifically, PFH and PFW measurements were significantly greater in the male group (9.680 ± 1.542 mm, 27.146 ± 2.689 mm, respectively) than in the female group (8.995 ± 1.494 mm, 25.884 ± 2.913 mm, respectively) (both $P < 0.001$). However, males had a shorter FPD (2.470 mm [3.658]) than females (3.051 mm [3.922]). Additionally, the male group had longer eyelids (UPML 35.830 ± 4.342 mm; LPML 29.762 ± 3.277 mm) than females (UPML 33.622 ± 4.417 mm; LPML 28.474 ± 3.246 mm). Moreover, the exposed ocular surface area in males was greater than that in females (2.069 ± 0.515 mm^2 and 1.895 ± 0.483 mm^2, respectively), and the male upper eyelid area (5.236 ± 1.179 mm^2) was smaller than that of females (6.153 ± 1.382 mm^2). However, there was no significant difference in CT and PFI between the sexes (all $P > 0.05$).

Table 3 Measurements difference between left and right eyes

Variable	Total ($N = 145$)				Male ($n = 48$)				Female ($n = 97$)			
	R	*L*	*t* value	*P* value	*R*	*L*	*t* value	*P* value	*R*	*L*	*t* value	*P* value
Linear dimensions(mm)												
PFH	9.086 ± 1.571	9.364 ± 1.505	−2.983	0.003*	9.582 ± 1.610	9.840 ± 1.470	−1.822	0.075	8.858± 1.518	9.111± 1.476	−2.304	0.023*
PFW	26.403 ± 2.836	26.212 ± 2.964	1.230	0.221	27.093 ± 2.902	27.199 ± 2.486	−0.337	0.708	26.023 ± 2.739	25.905 ± 2.787	0.752	0.454
FPD	2.973 (3.894)	2.967 (3.807)	–	0.128	2.759 (3.691)	1.622 (3.282)	–	0.155	2.896(3.884)	3.014(3.789)	–	0.396
Curve length (mm)												
UPML	34.539 ± 4.533	34.186 ± 4.894	1.597	0.113	36.022 ± 4.493	35.637 ± 4.224	1.162	0.251	33.790 ± 4.389	33.453 ± 4.462	1.166	0.246
LPML	28.904 ± 3.365	28.909 ± 3.260	−0.031	0.975	29.832 ± 3.365	29.693 ± 3.220	−0.438	0.663	28.435 ± 3.284	28.513 ± 3.224	−0.414	0.679
Angle (°)												
CT	170.763 ± 3.898	170.810 ± 4.298	−0.105	0.916	171.107 ± 4.214	171.593 ± 4.542	−0.615	0.542	170.590 ± 3.740	170.415 ± 4.138	0.324	0.747
Indices												
PFI	0.344 ± 0.051	0.356 ± 0.049	−3.060	0.003*	0.354 ± 0.054	0.362 ± 0.050	−1.129	0.102	0.341± 0.048	0.352 ± 0.049	−2.652	0.009*
Sizes (mm2)												
Upper eyelid area	5.815 ± 1.353	5.841 ± 1.338	−0.877	0.705	5.194 ± 1.137	5.279 ± 1.134	−0.743	0.461	6.123± 1.351	6.183 ± 1.418	−0.261	0.141
Ocular surface area	1.97165 ± 0.503	1.934 ± 0.498	1.129	0.232	2.097 ± 0.525	2.042 ± 0.509	0.990	0.327	1.910± 0.050	1.881± 0.486	0.029	0.450

R: Right eyes; *L*: Left eyes; PFH, Palpebral fissure height; PFW, Palpebral fissure width; FPD, Upper lid fold-palpebral margin distance; UPML, Upper palpebral margin length; LPML, Lower palpebral margin length; CT, Canthal tilt; PFI, Palpebral fissure index. Paired sample *t*-tests, except that FPD was analyzed by Wilcoxon signed-rank tests. *$P \leq 0.05$; **$P \leq 0.001$

Table 4 Variable measurement differences between different gender

Variable	M	F	*P*
Linear dimensions			
PFH	9.680 ± 1.542	8.995 ± 1.494	< 0.001**
PFW	27.146 ± 2.689	25.884 ± 2.913	< 0.001**
FPD	2.470 (3.658)	3.051 (3.922)	0.016*
Curve length			
UPML	35.830 ± 4.342	33.622 ± 4.417	< 0.001**
LPML	29.762 ± 3.277	28.474 ± 3.246	0.002*
Angle			
CT	171.350 ± 4.365	170.502 ± 3.934	0.098
Indices			
PFI	0.358 ± 0.053	0.349 ± 0.059	0.251
Sizes			
Upper eyelid area	5.236 ± 1.179	6.153 ± 1.382	< 0.001**
Ocular surface area	2.069 ± 0.515	1.895 ± 0.483	0.005*

M, male; F, female; PFH, Palpebral fissure height; PFW, Palpebral fissure width; FPD, Upper lid fold-palpebral margin distance; UPML, Upper palpebral margin length; LPML, Lower palpebral margin length; CT, Canthal tilt; PFI, Palpebral fissure index. Independent samples *t*-test, except that FPD was analyzed by Mann–Whitney U test. *$P \leq 0.05$; **$P \leq 0.001$

Correlation Between Age and Periocular Parameters

In the male group, PFW ($R = -0.523$, $P < 0.001$) and LPML ($R = -0.514$, $P = 0.264$) were moderately correlated with age, whereas the correlation between UPML and age was weak ($R = -0.367$, $P = 0.010$) (Fig. 2). Similarly, in the female group, a moderate correlation was observed between age and PFW ($R = -0.566$, $P < 0.001$) as well as age and LPML ($R = -0.537$, $P < 0.001$). Furthermore, PFH ($R = -0.315$, $P = 0.002$), UPML ($R = -0.381$, $P < 0.001$), and ocular surface area ($R = -0.457$, $P < 0.001$) showed a weak correlation with age of female (Fig. 3).

Discussion

Conventionally the direct anthropometry and 2D systems are standard methods for eyelids and brows related parameters measuring [10]. Direct anthropometry, which uses sliding and spreading calipers, is time-consuming and requires patient cooperation, while the 2D system, which allows for indirect anthropometry, requires labeling facial landmarks, attaching a ruler to the patient's face as a reference, and capturing images with different gazes [11]. Facial imaging contains more feature information of patients with dermatochalasis. Over the last decade, 3D imaging has become an area of interest in facial imaging, gradually replacing 2D systems and traditional anthropometry. Several studies have been devoted to the reliability, reproducibility, and accuracy

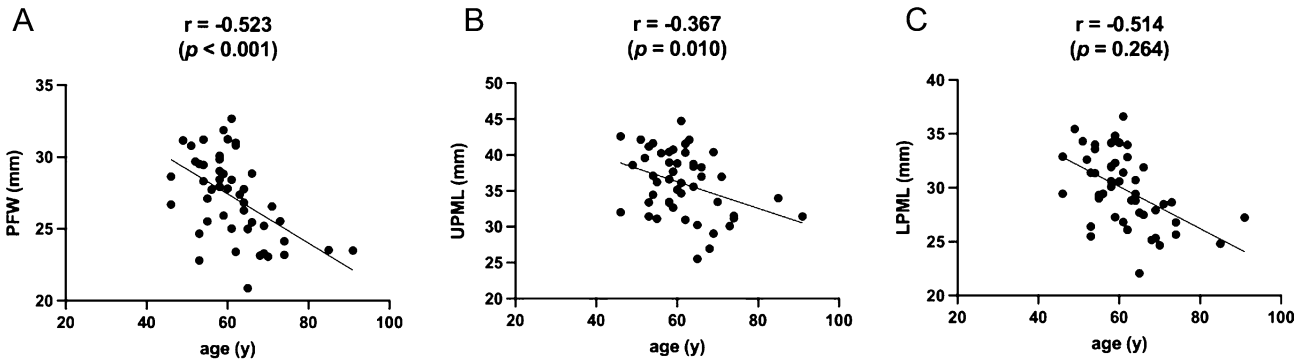

Fig. 2 Correlations between the periocular variables and age in males. **A** The correlation between palpebral fissure width (PFW) and age (Pearsons's correlation coefficient = −0.523). **B** The correlation between upper palpebral margin length (UPML) and age (Pearson's correlation coefficient = −0.367). **C** The correlation between lower palpebral margin length (LPML) and age (Pearson's correlation coefficient = −0.514).

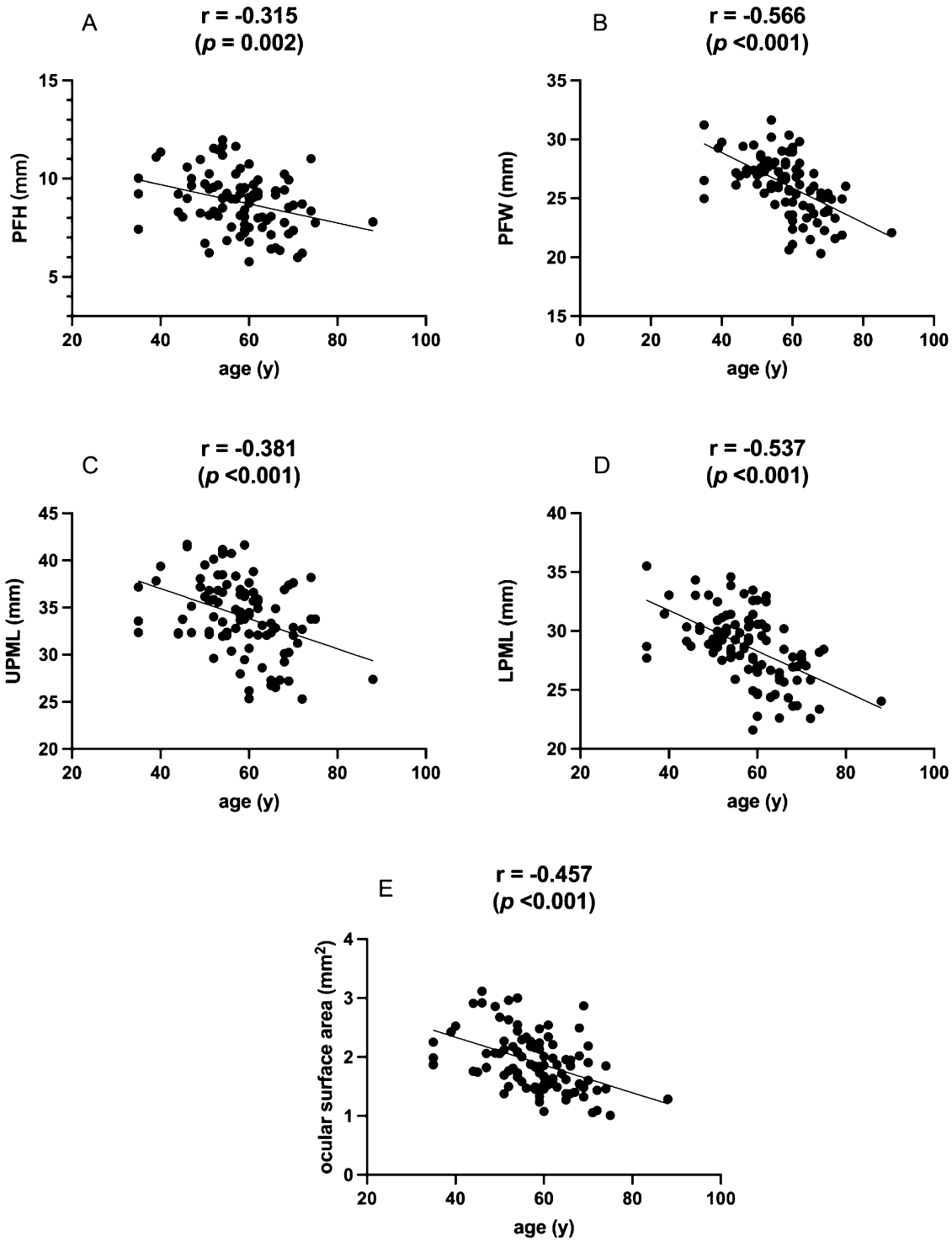

Fig. 3 The correlation between the periocular variables and age in females. **A** The correlation between palpebral fissure height (PFH) and age (Pearson's correlation coefficient = −0.315). **B** The correlation between palpebral fissure width (PFW) and age (Pearson's correlation coefficient = −0.566). **C** The correlation between upper palpebral margin length (UPML) and age (Pearson's correlation coefficient = −0.381). **D** The correlation between lower palpebral margin length (LPML) and age (Pearson's correlation coefficient = −0.537). **E** The correlation between ocular surface area and age (Pearson's correlation coefficient = −0.457).

of 3D photogrammetry in soft tissue evaluation [12–15], 3D stereophotogrammetry seems to be an optimal and accurate tool, especially for measuring the depth of facial sculptures [16, 17] and representing the texture and color of skin [15, 18]. Additionally, 3D imaging methods can provide measurements of linear distance, angle, size, and volume, as well as a permanent record of consultations [19]. In this study, we used the 3D stereophotogrammetry to analyze bilateral periocular regions of patients with dermatochalasis and evaluated age-dependent changes, the factors strongly associated with PFW and LPML are demonstrated.

Left–right bilateral symmetry is considered as an important aspect of creating beauty. Our study showed that PFH was more extensive on the left side than on the right side. As there was no significant difference in PFW, PFI was also greater on the left side. Except for PFH and PFI, no significant differences were noted in other parameters such as FPD, UPML and LPML, CT angles, upper eyelid area, and ocular surface area. The prevalence of asymmetry varies according to measurement criteria. In our study, the difference in PFH between the left and right sides was less than 1 mm, consistent with previously described differences in perceived asymmetry [20, 21]. Our findings also align with the work by Pool et al., which used 2D photo-assisted analysis and found no significant difference in the mean eyelid fissure height between the right and left eyes [22]. Our observations verified that patients with dermatochalasis exhibit bilateral symmetry in the periocular area.

Our study identified statistically significant sex-based differences in the manifestation of dermatochalasis. Specifically, we found that females had narrower PFH and PFW, longer FPD, shorter eyelid length, larger upper eyelid area, and smaller ocular surface area than males. These differences may be attributed to sex-based variations in tarsal plate size and axial ocular globe projection [23]. Our findings are consistent with those reported in other racial and ethnic groups, e.g., narrower PFW has also been documented in South Indian and Chinese females [24–26]. These differences highlight the importance of considering sex-related variances in upper eyelid morphology during blepharoplasty. Women generally have a larger upper eyelid area and a longer double eyelid fold than men, resulting in relatively smaller PFH and ocular surface area. Therefore, caution is necessary when removing excess skin; the amount might be less than that for men to avoid creating an excessively large PFH and ocular surface area, which could lead to an unnatural or "operated" appearance.

Age is widely recognized as the primary risk factor for sagging eyelids, as skin redundancy increases with age, leading to protrusion or drooping of the upper eyelids below the eyelashes [27–29]. Both genetic factors and extrinsic mechanisms such as chronic sunlight exposure, alcohol consumption, smoking, and nutritional deficiencies have been reported to influence skin aging [30]. The facial skeleton provides the structural framework for the overlying soft tissues. Notably, the process of facial skeleton resorption in the periorbital region, specifically involving the superomedial and inferolateral aspects of the orbit [31], leads to the movement of the location of the attachments of facial ligaments and muscles through the periosteum [32]. With advancing age, women experience an increase in both bony orbital volume and anterior globe position, while these measurements remain stable in men [33]. Muscular imbalance, loss of supportive structure volume, and drooping of the upper and midfacial feature could contribute to age-related changes in the periorbital region. In previous studies, sagging of eyelids was assessed using a 4-level Photonumerical Severity Scale, which classified the severity of sagging based on the relative position of the upper eyelid skin and the eyelashes [34]. Our study instead used a quantitative approach to present the severity of dermatochalasis by measuring periocular parameters. Our findings indicated that PFW and LPML were particularly susceptible to the effects of aging in both men and women. Moreover, UPML was noted to decrease slightly with age in the male group, and slight reductions of PFH, UPML, and ocular surface area occurred with age in the female group.

The PFW decreases in older individuals, likely due to increased skin laxity at the lateral and medial canthal tendon, causing a narrowing of the palpebral fissure. The minimal change in PFH is attributed to slightly weaker skin laxity in the central area compared to the periphery. When comparing between different ethnic populations, we found that reduced PFW was also documented in Korean and Turkish females: Kwon et al. [35] reported that Korean females over 60 years of age had the smallest PFH and PFW compared with younger or middle-aged females, and Direk et al. [36] found that Turkish females over 60 years of age had shorter PFH and narrower PFW compared with younger and middle-aged females. However, these studies did not include male participants. Additionally, these associations were only shown for the age group as a whole; a linear relationship with age was not demonstrated. Similarly, Raschke et al. [37] studied age-related anthropometric changes in Caucasians, but their findings were restricted to the perioral region. Park et al. demonstrated age-dependent shrinkage of the exposed corneal surface; however, their method involved qualitative analysis of 2D digital pictures and relied on the assumption that the pupil in each image was perfectly round. Moreover, PFH remains relatively stable with age, while LPML undergoes significant changes, indicating the laxity of the lower eyelid skin and the medial and lateral canthal tendons over time. This leads to a tendency for more ectropion rather than ptosis.

Based on our findings, strategic planning for operations should consider customized age and gender-specific techniques for blepharoplasty to preserve a natural and age-appropriate appearance.

In the preoperative phase of eyelid plastic surgery, in addition to comprehensive medical history evaluation and clinical examination, surgeons usually perform preoperative photography. This process involves identifying redundant upper eyelid skin, documenting any asymmetries, and so on. Our study emphasizes the importance of paying sufficient attention to the eye contour, especially in elderly patients with dermatochalasis. Regardless of gender, older patients should undergo a thorough assessment of eyelid laxity before surgery, which may include tests like the snap-back and pull-away tests. Especially the patients with eyelid skin laxity, it is essential to consider the condition of their inner and outer canthal ligaments. The decision to perform lateral canthopexy should be carefully considered, potentially addressing all symptoms in one surgery. During blepharoplasty, special attention should be given to the skin near the lateral canthus, and the amount of resection may need adjustment. Furthermore, as patients age, it becomes increasingly crucial to focus on postoperative complications, particularly lower eyelid malposition.

In our study, there are certain limitations that need to be acknowledged. Some studies define the upper eyelid not by the inferior margin of the brow but by the superior orbital rim [38]. However, in the case of the photograph, identifying the orbital rim beneath superficial tissue may lead to inaccuracies, especially in patients with dermatochalasis. Moreover, our objective is to measure the entire upper eyelid, and it is evident that demarcating below the orbital rim only represents a portion of the upper eyelid. But some patient's eyebrow shape contour may be not very clear. To enhance precision and reduce inter-patient variability, we have standardized the area measurement by incorporating eight points along the inferior margin of the eyebrow for each patient. This approach aims to minimize errors and variations among patients as effectively as possible. Additionally, it is important to note an imbalance in the gender distribution of our participants, with more females than males. This disparity may be due to increased concern about appearance and a higher willingness among women to undergo blepharoplasty compared to men. Furthermore, our study focused solely on pre-surgery patients and their characteristics; post-surgery data were not included in the current study. Finally, this paper solely examines the Caucasian ethnicity, which entails certain racial limitations, and suggests the need for future research involving a broader range of ethnic groups. These factors should be taken into consideration when interpreting our results.

In future investigations, we aspire to address these limitations by including a more balanced representation of male participants. Additionally, we intend to delve deeper into the post-surgery changes following blepharoplasty, employing 3D imaging for a comprehensive analysis in different races.

Conclusions

Our study of periocular characteristics in patients with dermatochalasis found that bilateral changes tended to appear simultaneously. Age was found to significantly affect certain periocular morphological changes, particularly the PFW and LPML. PFI did not appear to be influenced by age or sex. Our study provides ophthalmologists with valuable resources to improve understanding of morphology associated with dermatochalasis, develop anti-aging cosmetic surgery plans, and evaluating postoperative results.

Funding This study was supported by the State Scholarship Fund from China Scholarship Council (Nr. 202006370027 to X.L.), and the National Natural Science Foundation of China (Nr. 82102346 to Y.G.).

Declarations

Conflict of interest The authors declared no potential conflicts of interest with respect to the research, authorship, and publication of this article.

Ethical Approval All procedures performed in studies involving human participants were in accordance with the Declaration of Helsinki (as revised in 2013). The study was approved by the Ethics Committee of REDACTED (approval number: 17–199).

Informed Consent Informed consent was taken from all individual participants.

References

1. Espinoza GM, Holds JB (2005) Evolution of eyelid surgery. Facial Plast Surg Clin N Am 13(4):505–510
2. Guo Y et al (2020) A simple standardized three-dimensional anthropometry for the periocular region in a European population. Plast Reconstr Surg 145(3):514e–523e
3. Guo Y et al (2021) A novel approach quantifying the periorbital morphology: a comparison of direct, 2-dimensional, and 3-dimensional technologies. J Plast Reconstr Aesthet Surg 74(8):1888–1899
4. Guo Y et al (2019) Reliability of periocular anthropometry using three-dimensional digital stereophotogrammetry. Graefes Arch Clin Exp Ophthalmol 257(11):2517–2531
5. Hou X et al (2021) A novel standardized distraction test to evaluate lower eyelid tension using three-dimensional

stereophotogrammetry. Quant Imaging Med Surg 11(8):3735–3748
6. Hou XY et al (2022) A modified 3D stereophotogrammetry-based distraction test for assessing lower eyelid tension. Int J Ophthalmol 15(11):1757–1764
7. Liu J et al (2021) Reliability of stereophotogrammetry for area measurement in the periocular region. Aesthet Plast Surg 45(4):1601–1610
8. Guo Y et al (2023) A novel standardized approach for the 3D evaluation of upper eyelid area and volume. Quant Imaging Med Surg 13(3):1686–1698
9. Liu J et al (2023) Age-related changes of the periocular morphology: a two- and three-dimensional anthropometry study in Caucasians. Graefes Arch Clin Exp Ophthalmol 261(1):213–222
10. Macdonald KI et al (2014) Eyelid and brow asymmetry in patients evaluated for upper lid blepharoplasty. J Otolaryngol Head Neck Surg 43(1):36
11. Kashkouli MB et al (2017) Periorbital facial rejuvenation; applied anatomy and pre-operative assessment. J Curr Ophthalmol 29(3):154–168
12. Dindaroğlu F et al (2016) Accuracy and reliability of 3D stereophotogrammetry: a comparison to direct anthropometry and 2D photogrammetry. Angle Orthod 86(3):487–494
13. Liu J et al (2021) Accuracy of 3-dimensional stereophotogrammetry: comparison of the 3dMD and Bellus3D facial scanning systems with one another and with direct anthropometry. Am J Orthod Dentofac Orthop 160(6):862–871
14. Mao B et al (2022) The accuracy of a three-dimensional face model reconstructing method based on conventional clinical two-dimensional photos. BMC Oral Health 22(1):413
15. Savoldelli C et al (2019) Accuracy, repeatability and reproducibility of a handheld three-dimensional facial imaging device: the Vectra H1. J Stomatol Oral Maxillofac Surg 120(4):289–296
16. Anas IY, Bamgbose BO, Nuhu S (2019) A comparison between 2D and 3D methods of quantifying facial morphology. Heliyon 5(6):e01880
17. Ueda N et al (2021) Assessment of facial symmetry by three-dimensional stereophotogrammetry after mandibular reconstruction: a comparison with subjective assessment. J Stomatol Oral Maxillofac Surg 122(1):56–61
18. Ding Y et al (2015) Combination of 3D skin surface texture features and 2D ABCD features for improved melanoma diagnosis. Med Biol Eng Comput 53(10):961–974
19. Meng T et al (2020) Identifying facial features and predicting patients of acromegaly using three-dimensional imaging techniques and machine learning. Front Endocrinol (Lausanne) 11:492
20. Song WC et al (2007) Asymmetry of the palpebral fissure and upper eyelid crease in Koreans. J Plast Reconstr Aesthet Surg 60(3):251–255
21. Karlin JN, Rootman DB (2020) Brow height asymmetry before and after eyelid ptosis surgery. J Plast Reconstr Aesthet Surg 73(2):357–362
22. Pool SM, van der Lei B (2015) Asymmetry in upper blepharoplasty: a retrospective evaluation study of 365 bilateral upper blepharoplasties conducted between January 2004 and December 2013. J Plast Reconstr Aesthet Surg 68(4):464–468
23. Bashour M, Harvey J (2000) Causes of involutional ectropion and entropion-age-related tarsal changes are the key. Ophthalmic Plast Reconstr Surg 16(2):131–141
24. Vasanthakumar P, Kumar P, Rao M (2013) Anthropometric analysis of palpebral fissure dimensions and its position in South Indian ethnic adults. Oman Med J 28(1):26–32
25. Wu XS et al (2010) Investigation of anthropometric measurements of anatomic structures of orbital soft tissue in 102 Young Han Chinese adults. Ophthalmic Plast Reconstr Surg 26(5):339–343
26. Li Q et al (2016) Normative anthropometric analysis and aesthetic indication of the ocular region for young Chinese adults. Graefes Arch Clin Exp Ophthalmol 254(1):189–197
27. Flament F et al (2020) Age-related changes to characteristics of the human eyes in women from six different ethnicities. Skin Res Technol 26(4):520–528
28. Sforza C et al (2009) Age- and sex-related changes in the soft tissues of the orbital region. Forensic Sci Int 185(1–3):115.e1-115.e8
29. Liu Y et al (2013) A 3-dimensional anthropometric evaluation of facial morphology among Chinese and Greek population. J Craniofac Surg 24(4):e353–e358
30. Guinot C et al (2002) Relative contribution of intrinsic vs extrinsic factors to skin aging as determined by a validated skin age score. Arch Dermatol 138(11):1454–1460
31. Kahn DM, Shaw RB Jr (2008) Aging of the bony orbit: a three-dimensional computed tomographic study. Aesthet Surg J 28(3):258–264
32. Mendelson B, Wong CH (2020) Changes in the facial skeleton with aging: implications and clinical applications in facial rejuvenation. Aesthet Plast Surg 44(4):1151–1158
33. Ugradar S et al (2022) Orbital aging: a computed tomography-based study of 240 orbits. Plast Reconstr Surg 150(3):536e–545e
34. Jacobs LC et al (2014) Intrinsic and extrinsic risk factors for sagging eyelids. JAMA Dermatol 150(8):836–843
35. Kwon SH et al (2021) Three-dimensional photogrammetric study on age-related facial characteristics in Korean females. Ann Dermatol 33(1):52–60
36. Direk FK et al (2016) Anthropometric analysis of orbital region and age-related changes in adult women. J Craniofac Surg 27(6):1579–1582
37. Raschke GF et al (2014) Perioral aging–an anthropometric appraisal. J Craniomaxillofac Surg 42(5):e312–e317
38. Hyer JN et al (2021) Validating three-dimensional imaging for volumetric assessment of periorbital soft tissue. Orbit 40(1):9–17

5. Discussion

The publication, titled *Quantifying Dermatochalasis Using 3-Dimensional Photogrammetry* enrolled 145 patients with periocular dermatochalasis [1]. We utilized a 3D imaging system to measure and analysed various linear dimensions, such as PFH, PFW, FPD, and curve lengths like UPML and LPML. Additionally, we assessed parameters such as the CT angle, PFI indices, the area of the upper eyelid, and ocular surface. Subsequently, we evaluated the characteristics of dermatochalasis in patients, considering factors like symmetry, gender, and age. The article revealed that dermatochalasis displays symmetrical changes in both eyes. The study strongly suggested that surgeons should pay close attention to the eye contour before conducting blepharoplasty. Moreover, surgical procedures should be tailored to include age- and gender-specific techniques to ensure a natural and age-appropriate appearance, as evidenced by our gender and age comparisons. Special care should be directed toward the skin near the lateral canthus. In post-operative follow-up, it is advisable for patients to regularly monitor potential complications, with a particular focus on lower eyelid malposition.

Our study conducted a detailed analysis of the periocular area in patients with dermatochalasis, excluding the volume of the upper eyelid. In our previous study, we employed a modified landmarks localization strategy to encircle the upper eyelid and measure its volume in healthy volunteers [19, 20]. And our results confirmed that directly circling the upper eyelid and measuring the volume of the selected area is not reliable. The decreased reliability can be attributed to the anatomical characteristics of the broad eyelid base and the absence of an efficient, fixed datum plane for volumetric measurements in the eyelid region [19]. Measuring volume and size holds promise in clinical settings, as surgeons can effectively assess changes in the surgical area after the procedure and simulate outcomes in the 3D system beforehand to determine the amount of skin and fat that needs removal. Several studies have explored volume measurement using 3D imaging systems. Crstel et al. [29] proposed that the Vectra XT 3D system

can accurately measure volume changes post-surgery, although they did not assess reliability and accuracy. Hyer et al. [30] reported that the Vectra M3 imaging system is accurate with good interobserver repeatability. However, they defined the periorbital area from the upper eyelid to the supraorbital rim when the healthy volunteer closes their eyes.

In future studies, we can explore different selected areas to assess the reliability of volume measurement. Simultaneously, we can evaluate variations across different human ethnicities using various 3D imaging systems. In addition, in the Vectra 3D imaging system, the surgeon can register a baseline 3D image, and then register subsequent 3D image base on the 3D image to achieve overlap both photos. For the dermatochalasis patients, the post- and pre- photos could be overlapped to evaluate if the volume calculation accurate and reliable. If this method is certified, the volume change could be calculated furtherly.

Besides the eyes and eyelids, eyebrows also play a significant role in human facial expression and aesthetic appearance. The ideal eyebrow position varies across different genders, races, ages, and generations. Typically, female eyebrows are positioned above the level of the bony superior orbital margin with an upward arch, so the brow peak lies between the lateral margin and the outer canthus. In contrast, male eyebrows are usually at or slightly above the upper orbital margin and have a flatter outline [31].

The brow position and morphology has been measured by different techniques. Normally, the vertical linear distance central-brow pupil height (CPBH) was measured [32, 33]. Some studies also calculated the ratio of midface proportion [34, 35]. Vertical lines from the medial palpebral fissure to brow height (MPBH) and from the lateral palpebral fissure to brow height (LPBH) were employed for accurate measurement of brow morphology [36-38]. To assess the position of different parts of the eyebrow, angular measurements were also taken in some study, like the acute angle between the vertical line containing the lateral canthal angle and the line including the outermost

point of the eyebrow and the lateral canthal angle [39-41]. However, we think this measurement has limitations since the position of the lateral canthal angle can change after blepharoplasty. Some studies have calculated the angle formed by the vertical line from the center of the pupil to the mid-brow and a line from the same point at the mid-brow to the lateral brow to explore brow position changes [42, 43]. In our previous studies, it was found that using the pupil as a stable reference plane to describe periocular changes is more reliable compared to using the endocanthion and exocanthion [44]. Hence, measure the angle based on the vertical line passing through the center of the pupil might be better.

The ideal eyebrow position is very important for the outcome of upper eyelid surgery. In blepharoplasty, the appropriate surgical technique is selected based on the patients' clinical manifestations and the surgeon's experience. Some patients with upper eyelid skin redundancy undergo excision of skin, fat tissue, and orbicularis. Others with senile or subclinical ptosis may undergo levator or Muller muscle aponeurosis plication, advancement, or resection. Many patients undergo double eyelid surgery to enhance their aesthetic appearance and increase the surface area of their eyes, particularly in Asian countries.

The position of the brow changes after different surgery procedure has been a subject of debate over the past decade. While some descending brows may correct themselves automatically several months later, others experience persistent brow ptosis. Xu et al. [34] evaluated patients who underwent primary double eyelid surgery in Asians and reported a lower brow position after the surgery. Zhang et al. [35] also reported a decrease in midface proportion from 0.801 to 0.698 six months after the surgery in Asians. Kokubu et al. [37] captured frontal portraits and close-up midface photographs, analyzing them with Adobe imaging software, and reported eyebrow dropping three months postoperatively.

To the best of our knowledge, most studies have analyzed brow changes using 2D

photos, and research on the correlation between upper eyelid changes and brow position is scarce. In our study, 3D photos could be further marked and analyzed for brow position and morphology in future research. Additionally, we could explore potential relationships between the size and volume changes of the upper eyelid and eyebrow alterations. These research findings have the potential to assist in the systematic preparation of upper eyelid blepharoplasty, aiming to achieve anticipated surgical outcomes and meet patients'expectations.

With the advancement of artificial intelligence (AI), AI technology is gradually being integrated into medical imaging processing and analysis. It is predicted that the appropriate clinical use of artificial intelligence tools, especially those involving image recognition, has the potential to enhance clinical efficiency [45]. Ferry et al. [46] introduced an automatic approach to extracting phenotypic information from 2D photos and used machine learning to analyze craniofacial dysmorphisms. To capture facial phenotypes more comprehensively, like 3D models [47], they not only focused on 36 facial feature points but also registered a person's face from multiple images over time. In Liu et al.'s study [48], AI was employed to quantify sexual dimorphism in aesthetic faces and identify gender characteristics. One limitation of this study was the use of 2D photos, which cannot provide detailed information such as identifying topographic differences between males and females. Pei et al. [49] utilize FaceGo pro (Revopoint, China) to generate 3D facial models for 669 patients. Through various machine learning algorithms, they predicted difficult mask ventilation in patients scheduled for general anesthesia. Likewise, 3D imaging photos, combined with machine learning, can also be applied in predicting obstructive sleep apnea [50], automating the diagnosis of fetal alcohol syndrome [51], and facilitating syndrome diagnosis [52].

Therefore, the 3D photos of patients with dermatochalasis in our study can not only be utilized for research on dermatochalasis before and after surgery but can also be further integrated with machine learning techniques for diagnosis and prediction in the future. By harnessing the power of 3D imaging and machine learning algorithms, we can

potentially enhance the accuracy and efficiency of diagnosing other disease, leading to more precise predictions and personalized treatment strategies.

6. References

1. Li, X., et al., Quantifying Dermatochalasis Using 3-Dimensional Photogrammetry. Aesthetic Plast Surg, 2023.
2. Mendelson, B. and C.H. Wong, *Changes in the facial skeleton with aging: implications and clinical applications in facial rejuvenation.* Aesthetic Plast Surg, 2012. **36**(4): p. 753-60.
3. Jacobs, L.C., et al., *Intrinsic and extrinsic risk factors for sagging eyelids.* JAMA Dermatol, 2014. **150**(8): p. 836-43.
4. Damasceno, R.W., et al., *Eyelid aging: pathophysiology and clinical management.* Arq Bras Oftalmol, 2015. **78**(5): p. 328-31.
5. Matiegka, J., *The testing of physical efficiency.* Am J Phys Anthropol, 1921. **4**(3): p. 223-30.
6. Guo, Y., et al., *Reliability of Periocular Anthropometry: A Comparison of Direct, 2-Dimensional, and 3-Dimensional Techniques.* Dermatol Surg, 2020. **46**(9): p. e23-e31.
7. Franke-Gromberg, C., et al., *Digital 2D-photogrammetry and direct anthropometry--a comparing study on test accomplishment and measurement data.* Anthropol Anz, 2010. **68**(1): p. 11-20.
8. Lim, Y.C., A.S. Abdul Shakor, and R. Shaharudin, *Reliability and Accuracy of 2D Photogrammetry: A Comparison With Direct Measurement.* Front Public Health, 2021. **9**: p. 813058.
9. Ayaz, I., et al., *Accuracy and reliability of 2-dimensional photography versus 3-dimensional soft tissue imaging.* Imaging Sci Dent, 2020. **50**(1): p. 15-22.
10. Jones, P.R., et al., *The Loughborough anthropometric shadow scanner (LASS).* Endeavour, 1989. **13**(4): p. 162-8.
11. Yang, Y., et al., *A Quantitative Three-Dimensional Tear Trough Deformity Assessment and Its Application in Orbital Septum Fat Transposition.* Aesthetic Plast Surg, 2023.
12. Yang, Y., et al., *Gender- and Age-Related Characterization of Lip Morphology:*

A Three-Dimensional Analysis in a Chinese Population. Aesthet Surg J, 2023.

13. Sowmya, M.V., et al., *3D assessment of ear morphology.* J Oral Biol Craniofac Res, 2023. **13**(5): p. 622-629.
14. Chen, G., et al., *Occlusion-Based Three-Dimensional Craniofacial Anthropometric and Symmetric Evaluation in Preadolescences: A Comparative COHORT Study.* J Clin Med, 2023. **12**(15).
15. Dallazen, E., et al., *Comparison of Manual (2D) and Digital (3D) Methods in the Assessment of Simulated Facial Edema.* J Oral Maxillofac Surg, 2023. **81**(9): p. 1146-1154.
16. Andrews, J., et al., *Validation of three-dimensional facial imaging captured with smartphone-based photogrammetry application in comparison to stereophotogrammetry system.* Heliyon, 2023. **9**(5): p. e15834.
17. Guo, Y., et al., *Reliability of periocular anthropometry using three-dimensional digital stereophotogrammetry.* Graefes Arch Clin Exp Ophthalmol, 2019. **257**(11): p. 2517-2531.
18. Liu, J., et al., *Reliability of Stereophotogrammetry for Area Measurement in the Periocular Region.* Aesthetic Plast Surg, 2021. **45**(4): p. 1601-1610.
19. Guo, Y., et al., *A novel standardized approach for the 3D evaluation of upper eyelid area and volume.* Quant Imaging Med Surg, 2023. **13**(3): p. 1686-1698.
20. Fan, W., et al., *Evaluation of the Portable Next-Generation VECTRA H2 3D Imaging System for Measuring Upper Eyelid Area and Volume.* Aesthet Surg J, 2023. **43**(10): p. 1114-1123.
21. Sobti, M. and N. Joshi, *Lower Eyelid Blepharoplasty: Minimizing Complications and Correction of Lower Eyelid Malposition.* Facial Plast Surg, 2023. **39**(1): p. 28-46.
22. Bonan, P., et al., *Laser-assisted blepharoplasty: An innovative safe and effective technique.* Skin Res Technol, 2023. **29**(5): p. e13351.
23. Carqueville, J.C. and C. Chesnut, *Histologic Comparison of Upper Blepharoplasty Skin Excision Using Scalpel Incision Versus Microdissection Electrocautery Needle Tip Versus Continuous Wave CO2 Laser.* Dermatol Surg,

2021. **47**(10): p. 1376-1378.

24. Patel, B.C., K. Volner, and R. Malhotra, *Transconjunctival Blepharoplasty*, in *StatPearls*. 2023, StatPearls Publishing Copyright © 2023, StatPearls Publishing LLC.: Treasure Island (FL).
25. Romeo, F., *Upper Eyelid Filling With or Without Surgical Treatment.* Aesthetic Plast Surg, 2016. **40**(2): p. 223-35.
26. Romeo, F., *Upper Eyelid Filling Approach [U.E.F.A.] Technique: State of the Art After 500 Consecutive Patients.* Aesthetic Plast Surg, 2019. **43**(3): p. 663-672.
27. Verner, I., H.P. Naveh, and S. Cotofana, *A novel ablative radiofrequency microplasma nonsurgical blepharoplasty for dermatochalasis.* Dermatol Ther, 2020. **33**(6): p. e14002.
28. Rossi, E., et al., *Clinical and Confocal Microscopy Study of Plasma Exeresis for Nonsurgical Blepharoplasty of the Upper Eyelid: A Pilot Study.* Dermatol Surg, 2018. **44**(2): p. 283-290.
29. Cristel, R.T. and B.P. Caughlin, *Lower Blepharoplasty Three-Dimensional Volume Assessment after Fat Pad Transposition and Concomitant Fat Grafting.* Facial Plast Surg, 2020. **36**(4): p. 478-483.
30. Hyer, J.N., et al., *Validating three-dimensional imaging for volumetric assessment of periorbital soft tissue.* Orbit, 2021. **40**(1): p. 9-17.
31. Patel, B.C. and R. Malhotra, *Mid Forehead Brow Lift*, in *StatPearls*. 2023, StatPearls Publishing Copyright © 2023, StatPearls Publishing LLC.: Treasure Island (FL).
32. Rootman, D.B., et al., *The Effect of Ptosis Surgery on Brow Position and the Utility of Preoperative Phenylephrine Testing.* Ophthalmic Plast Reconstr Surg, 2016. **32**(3): p. 195-8.
33. Nakra, T., et al., *The effect of upper eyelid blepharoplasty on eyelid and brow position.* Orbit, 2016. **35**(6): p. 324-327.
34. Xu, L., et al., *Aesthetic Analysis of Alteration of Eyebrow Position After Double Eyelidplasty.* Aesthetic Plast Surg, 2020. **44**(2): p. 373-378.

35. Zhang, Y. and Z. Xiao, *Upper Eyelid Blepharoplasty Improved the Overall Periorbital Aesthetics Ratio by Enhancing Harmony Between the Eyes and Eyebrows.* Clin Cosmet Investig Dermatol, 2022. **15**: p. 1969-1978.
36. Hassanpour, S.E. and H. Khajouei Kermani, *Brow Ptosis after Upper Blepharoplasty: Findings in 70 Patients.* World J Plast Surg, 2016. **5**(1): p. 58-61.
37. Kokubo, K., et al., *Evaluation of the eyebrow position after levator resection.* J Plast Reconstr Aesthet Surg, 2017. **70**(1): p. 85-90.
38. Rubinstein, T.J., et al., *Preoperative phenylephrine testing as a predictor of postoperative eyebrow position.* Int J Ophthalmol, 2016. **9**(3): p. 472-4.
39. Prado, R.B., et al., *Assessment of eyebrow position before and after upper eyelid blepharoplasty.* Orbit, 2012. **31**(4): p. 222-6.
40. Matai, O., et al., *[Evaluation of eyebrow position using angular measures]*. Arq Bras Oftalmol, 2007. **70**(1): p. 41-4.
41. Sadacharan, C.M. and V. Packirisamy, *Photogrammetric Analysis of Eyebrow and Eyelid Dimensions in Indian American Adults.* J Craniofac Surg, 2020. **31**(8): p. e796-e800.
42. Yoon, N.S. and H.B. Ahn, *Exploring Brow Position Changes with Age in Koreans.* Korean J Ophthalmol, 2019. **33**(1): p. 91-94.
43. Glass, L.R., et al., *The lateral brow: position in relation to age, gender, and ethnicity.* Ophthalmic Plast Reconstr Surg, 2014. **30**(4): p. 295-300.
44. Liu, J., et al., *Age-related changes of the periocular morphology: a two- and three-dimensional anthropometry study in Caucasians.* Graefes Arch Clin Exp Ophthalmol, 2023. **261**(1): p. 213-222.
45. Davenport, T. and R. Kalakota, *The potential for artificial intelligence in healthcare.* Future Healthc J, 2019. **6**(2): p. 94-98.
46. Ferry, Q., et al., *Diagnostically relevant facial gestalt information from ordinary photos.* Elife, 2014. **3**: p. e02020.
47. Hammond, P., et al., *Discriminating power of localized three-dimensional facial morphology.* Am J Hum Genet, 2005. **77**(6): p. 999-1010.

48. Liu, A.S., C.A. Salinas, and B.A. Sharaf, *Using Artificial Intelligence to Quantify Sexual Dimorphism in Aesthetic Faces: Analysis of 100 Facial Points in 42 Caucasian Celebrities.* Aesthet Surg J Open Forum, 2023. **5**: p. ojad046.

49. Pei, B., et al., *Geometric morphometrics and machine learning from three-dimensional facial scans for difficult mask ventilation prediction.* Front Med (Lausanne), 2023. **10**: p. 1203023.

50. Monna, F., et al., *Machine learning and geometric morphometrics to predict obstructive sleep apnea from 3D craniofacial scans.* Sleep Med, 2022. **95**: p. 76-83.

51. Fang, S., et al., *Automated diagnosis of fetal alcohol syndrome using 3D facial image analysis.* Orthod Craniofac Res, 2008. **11**(3): p. 162-71.

52. Hallgrímsson, B., et al., *Automated syndrome diagnosis by three-dimensional facial imaging.* Genet Med, 2020. **22**(10): p. 1682-1693.

53. *VECTRA M3 3D Imaging System | Canfield Scientific*. (Access on 2023.10.29). https://www.canfieldsci.com/imaging-systems/vectra-m3-3d-imaging-system/

7. Appendix

Figure legends

1. Figure 1. Dermatochalasis Patients Captured Using the VECTRA M3 Imaging System
2. Figure 2. VECTRA M3 dimensions
3. Figure 3. Pre-intra-post-operative clinical pathway.

   Prior to surgery, patients underwent detailed consultations for clinical history, clinical evaluation, and 3D imaging. The blepharoplasty procedure involved anesthesia, excision and dissection, fat resection, and suturing. After surgery, patients received careful postoperative care and were scheduled for follow-up appointments at 1 week, 1 month, and 3 months post-surgery. Additionally, 3D photos were taken during the 3-month period after the surgery.

8. Vorabveröffentlichungen von Ergebnissen